Resilience-Driven System Design of Complex Engineered Systems

Byeng D. Youn[1]

Assistant Professor
School of Mechanical and Aerospace
Engineering Seoul National University,
Seoul 151-742, Korea
e-mail: bdyoun@snu.ac.kr

Chao Hu

Department of Mechanical Engineering,
University of Maryland at
College Park, College Park, MD 20742
e-mail: huchaost@umd.edu

Pingfeng Wang

Assistant Professor
Department of Industrial and Manufacturing
Engineering, Wichita State University,
Wichita, KS 67260
e-mail: pingfeng.wang@wichita.edu

Most engineered systems are designed with a passive and fixed design capacity and, therefore, may become unreliable in the presence of adverse events. Currently, most engineered systems are designed with system redundancies to ensure required system reliability under adverse events. However, a high level of system redundancy increases a system's life-cycle cost (LCC). Recently, proactive maintenance decisions have been enabled through the development of prognostics and health management (PHM) methods that detect, diagnose, and predict the effects of adverse events. Capitalizing on PHM technology at an early design stage can transform passively reliable (or vulnerable) systems into adaptively reliable (or resilient) systems while considerably reducing their LCC. In this paper, we propose a resilience-driven system design (RDSD) framework with the goal of designing complex engineered systems with resilience characteristics. This design framework is composed of three hierarchical tasks: (i) the resilience allocation problem (RAP) as a top-level design problem to define a resilience measure as a function of reliability and PHM efficiency in an engineering context, (ii) the system reliability-based design optimization (RBDO) as the first bottom-level design problem for the detailed design of components, and (iii) the system PHM design as the second bottom-level design problem for the detailed design of PHM units. The proposed RDSD framework is demonstrated using a simplified aircraft control actuator design problem resulting in a highly resilient actuator with optimized reliability, PHM efficiency and redundancy for the given parameter settings. [DOI: 10.1115/1.4004981]

Keywords: resilience, reliability, complex engineered systems, prognostics and health management

1 Introduction

In the past few decades, reliability has been widely recognized as of great importance in engineering product and process design. Hence, considerable advances have been made in the field of reliability-based design optimization (RBDO) [1–6] for engineered system reliability analysis and design while taking into account various variability sources (e.g., material properties, loads, and geometric tolerances). Additionally, advanced numerical methods for reliability assessment have been proposed to enhance numerical efficiency and stability [6–10]. In RBDO, reliability is defined as the probability that a system performance (e.g., fatigue, corrosion, and fracture) meets its marginal value under variability. Although reliability-based design can improve system reliability to some degree, most engineered systems can only be designed with a passive and fixed design capacity—the load level that the system design can withstand—and, therefore, may become unreliable in the presence of adverse events.[2] To maintain the desired level of system reliability under adverse events, a great deal of system redundancy is designed into most engineered systems, resulting in a strikingly high life-cycle cost (LCC) to be incurred in development, operation, and maintenance processes.

Recently, prognostics and health management (PHM) methods have been developed to detect, diagnose, and predict the system-wide effects of adverse events. *Condition monitoring* (CM) is the process of diagnosing health conditions based on sensory signals and related health measures. Popular tools used for CM include statistical methods [11,12] and artificial intelligence, such as neural networks and fuzzy logic [13,14]. CM has been applied to various engineering applications, including: machine components [15,16], machine tools [17,18], and power generator/transformers [19–21]. *Real-time prognostics* research has been conducted with an emphasis on modeling the remaining useful life (RUL) distribution and reliability. In general, prognostics approaches can be categorized into model-based approaches [22–24], data-driven approaches [25–27] and hybrid approaches [28,29]. PHM research has been conducted with various systems, such as light-emitting diodes [30,31], civil systems [32], and fuel cells [33]. *Condition-based maintenance* (CBM) is the maintenance decision process that exploits CM and prognostics information to maximize the availability of the system and to minimize its long-run expected cost. Component replacement in this maintenance is triggered when the system condition reaches a threshold condition or the owner's cost is minimal [34–36]. It is noted that PHM has been successful, in part, in lowering system maintenance costs. In addition, it was reported that PHM may have the capability to make engineered systems highly reliable with a reduced level of redundancy [37]. However, it has not been used as a means to adaptively ensuring high system reliability under adverse conditions. Capitalizing on PHM technology at an early design stage may enable the transformation of passively reliable (or vulnerable) conventional systems into adaptively reliable (or resilient) complex systems while considerably reducing systems' LCCs. There is, however, no definition and mathematical framework of engineering resilience to take advantage of PHM because the two interrelated disciplines (engineering reliability and PHM) have, to date, been developed in parallel and independently.

The above literature survey reveals a great potential for the advancement of PHM technology together with the system reliability technology to further make engineered systems resilient.

---

[1]Corresponding author.

[2]Adverse events could include the failure of components due to internal hazards (e.g., degradation) and/or external hazards (e.g., harsh operational conditions) that occur during the mission of the systems.

This study aims at exploiting this potential to incorporate the resilience concept into engineering design and to transform the conventional RBDO to resilience-driven system design (RDSD). This design framework is composed of three hierarchical tasks, namely the resilience allocation problem (RAP) as a top-level design problem to define a resilience measure as a function of reliability and PHM efficiency in an engineering context, the system reliability-based design optimization (RBDO) as the first bottom-level design problem for the detailed design of components, and the system PHM design as the second bottom-level design problem for the detailed design of PHM units. We expect that the resulting system design is capable of detecting, anticipating and recovering from adverse events.

The paper is organized as follows. Section 2 reviews the research in resilience and introduces the concept of resilience to a complex engineered system. The notions detection, anticipation, and recovery are situated in this context. Section 3 presents the hierarchical RDSD framework along with detailed design and analysis problems. Section 4 reports the results of an engineering case study to illustrate the proposed framework. The paper is concluded in Sec. 5.

2 Resilience Concept

Many developments have been achieved in the research on resilience in several nonengineering fields. However, resilience in engineering design remains almost untouched. There is still a great need for a theoretical basis that furnishes a better understanding of how engineered systems achieve resilience, as well as enables the development of a generic resilience principle widely applicable to the field of engineering design. This section first provides a brief review of the research on resilience in nonengineering fields, and then presents a mathematical definition of engineering resilience along with its generic formula.

2.1 Research on Resilience. In recent years, research on resilience has been widely conducted in ecology [38–40], psychology [41–44], economics and organizational science [45–47], and others to improve the ability of systems or people to respond to and quickly recover from catastrophic events.

In ecology, resilience is loosely defined as "the ability of the system to maintain its function when faced with novel disturbance" [38]. The current research on resilience applied to ecosystems mainly focuses on the analysis of ecosystem resilience using complex adaptive systems (CAS) theory [39]. As an extension of traditional systems theory, the CAS theory enables analysis of the role of adaptation in system resilience through specifically modeling how individual variation and changes in that variation lead to system-level responses [39]. Furthermore, natural selection and evolution plays an important role in shaping ecological response to disturbance, which provides new insight to the understanding of resilience [40]. In psychology, resilience is defined as a dynamic process that individuals exhibit positive behavioral adaptation when they encounter significant adversity [41]. The process of resilience involves both the exposure of adversity and the positive adaptation to that adversity. Extensive

research has been conducted to understand the protective factors that contribute to people's adaptation to adverse conditions, e.g., bereavement [42], terrorist attacks [43], or urban poverty [44].

In economics and organizational science, resilience of an organization can be defined as its intrinsic ability to keep or recover a stable state, thereby allowing it to continue operations after a disruption or in presence of continuous stress [45,46]. In economics, resilience can be improved by adding redundancy or increasing flexibility. While investments in redundancy means a pure increase in cost, investments in flexibility yields many competitive advantages in day-to-day operations [45]. Of particular interest here is the characterization of a resilient organization with the following three steps within the context of a perturbation, as shown in Fig. 1 [47]. First, the organization should continuously monitor key state variables indicative of its health condition to anticipate the occurrence of a perturbation. Second, upon the occurrence of a perturbation, the system should conduct the situation assessment and identify an optimal way to reorganize itself and keep operations. Third, after the occurrence of a perturbation, the organization should analyze various alternative ways of functioning and learn from the past experiences to determine the most relevant state variables for the first step and to enhance its capability to cope with perturbations.

In contrast to the aforementioned developments of resilience in many nonengineering fields, resilience in engineering design has rarely been studied. One possible reason is that PHM, which is essential to make engineered systems resilient, has only recently received critical attention from the research community. It is fair to say, therefore, that there is still a great need for a theoretical basis that furnishes a better understanding of how engineered systems achieve resilience, as well as enables the development of an engineering resilience principle readily applicable to engineering design.

2.2 Definition of Engineering Resilience. This subsection aims at proposing a conceptual definition of engineering resilience, which will facilitate the derivation of its generic formula in terms of reliability and other key PHM attributes. Nonresilient system designs encounter gradual degradation of system capacity and performance due to adverse events (see Fig. 2(a)). In contrast, resilient system designs will be able to recover from their critical health states by restoring the system capacity (see Fig. 2(b)). PHM will support logical decisions about when and how to restore the system capacity. The capacity restoration (ρ) can be defined as the degree of reliability recovery. It can be found that the restoration is a joint probability of a system failure event (E_{sf}), a correct diagnosis event (E_{cd}), a correct prognosis event (E_{cp}), and an mitigation/recovery (M/R) action success event (E_{mr}), expressed as

$$\rho(R, \Lambda_P, \Lambda_D, \kappa) \triangleq \Pr(E_{sf} E_{cd} E_{cp} E_{mr}) = \Pr(E_{mr}|E_{cp}E_{cd}E_{sf}) \cdot \\ \Pr(E_{cp}|E_{cd}E_{sf}) \cdot \Pr(E_{cd}|E_{sf}) \cdot \Pr(E_{sf}) \\ = \kappa \cdot \Lambda_P \cdot \Lambda_D(1 - R)$$

(1)

where κ, Λ_P, and Λ_D are the conditional probabilities of the M/R action success, correct prognosis and diagnosis, and $(1 - R)$ is the
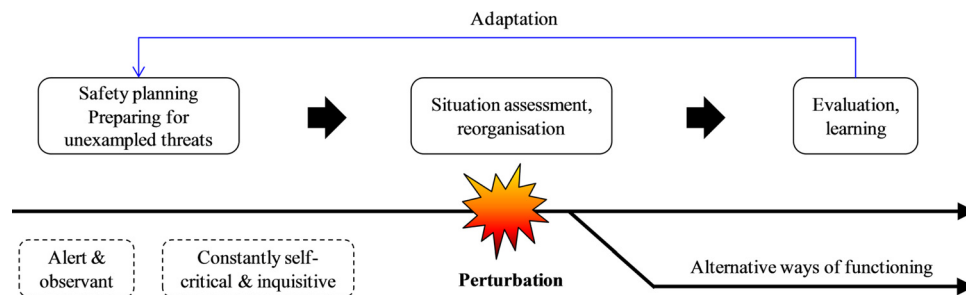

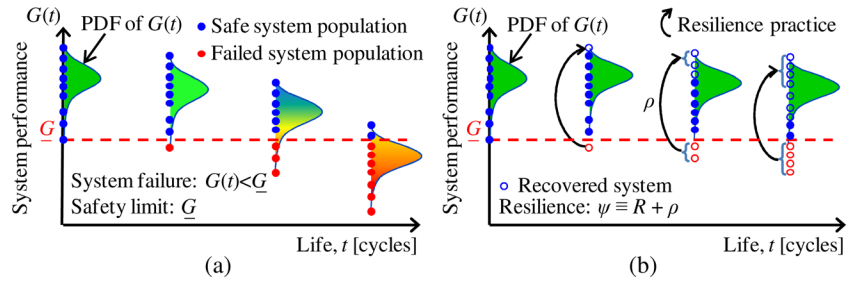**Fig. 1 Resilient (Proactive) organization**

Fig. 2 System performance changes over lifetime without (*a*) and with the resilience practice (*b*)

probability of system failure. In this study, the value of κ is held constant here by assuming that M/R maintenance actions are consistently performed. However, there is no restriction on the form of κ. In particular, κ can be a nonlinear function of the system reliability R, indicating that the performance of an M/R action is affected by the health condition of the engineered system.

The conceptual definition of engineering resilience is the degree of a passive survival rate (or reliability) plus a proactive survival rate (or restoration). Mathematically, the resilience measure can be defined as the addition of reliability and restoration as (see Fig. 2(*b*))

$$\text{Resilience } (\Psi) \triangleq \text{Reliablity}(R) + \text{Restoration } (\rho) \rightarrow \Psi$$
$$\triangleq R + \rho(R, \Lambda_P, \Lambda_D, \kappa) \tag{2}$$

It is noted that the above definition turns engineering resilience to a quantifiable property, making it possible to analyze the resilience potential of an engineered system. In what follows, we intend to further elaborate on the two hallmarks of engineering resilience: reliability and restoration.

Reliability: Reliability quantifies the ability of an engineered system to maintain its capacity and performance above a safety limit during a given period of time under stated conditions. Accordingly, resilience is characterized by preserving an acceptable level of capacity and performance despite adverse events. We note that reliability should be treated as an important system characteristic that contributes to engineering resilience from the perspective of system self-preservation. Conventional RBDO practice endeavors to pursue high reliability with low cost through cost minimization under stringent reliability constraints [1–6].

Restoration: Restoration measures the ability of an engineered system to restore its capacity and performance by detecting, predicting, and mitigating or recovering from the system-wide effects of adverse events. It can be viewed as the adaptability of an engineered system to its changing performance and capacity due to adverse events. This adaptability enables an adaptive reliability throughout the system's lifetime.
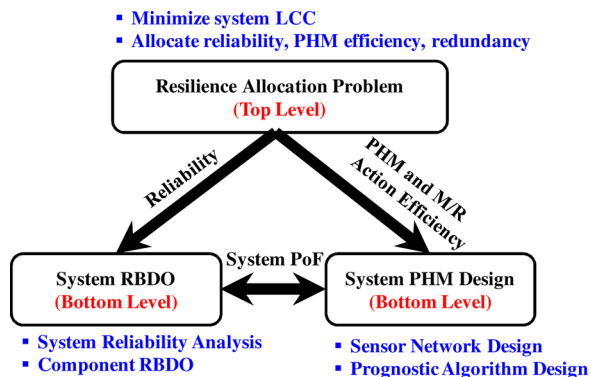
From the perspective of conventional engineering reliability, the failure of an engineered system typically refers to a breakdown or malfunctioning of the system and/or its components. This view assumes that success or failure is only an observable consequence that does not necessarily reflect the system's characteristic of adaptation. From the perspective of engineering resilience, however, success is due to the ability of an engineering system to make right adjustments in a timely manner, in particular to anticipate failures before they occur. Failure is due to the absence of that ability—either temporarily when the system performance falls below the safety limit or permanently. Reliability and restoration works in a highly cooperative manner to build the system's resilience. System design must encompass enhancing this cooperative strength, rather than just reducing the probability of failure. The framework of system design with this purpose will be discussed in detail in Sec. 3.

3 Framework of Resilience-Driven System Design

This section presents the proposed framework of resilience-driven system design. Section 3.1 provides an overview of this framework which consists of one top-level and two bottom-level design problems. Section 3.2 details the top-level design problem, namely the resilience allocation problem (RAP). Section 3.3 is dedicated to introducing the first bottom-level design problem for the detailed design of components, namely the system RBDO. Following the first bottom-level design problem, the detailed PHM design is determined in the second bottom-level design problem, namely, the system PHM, which is thereafter detailed in Sec. 3.4.

3.1 Overview of Resilience-Driven System Design. We begin with an overview of the resilience-driven system design framework. This framework is composed of three hierarchical design tasks (see Fig. 3), namely the resilience allocation problem (RAP) as a top-level design problem to define a resilience measure as a function of reliability and PHM efficiency in an engineering context, the system RBDO as a bottom-level design problem for the detailed design of components, the system PHM design as a bottom-level design problem for the detailed design of PHM units.

The bottom level design problems, the system RBDO and the system PHM design, should be solved interactively. However, since optimal design of PHM units depends on failure mechanisms and layouts of components, it is noted that PHM units must be designed upon the completion of initial component design. Therefore, the RBDO problem will be solved first and then the system PHM design will be conducted. The results from the PHM design will be used to refine the solution of the RBDO problems iteratively if necessary. Depending on the design results, the iterative process between the system RBDO and the PHM design might be needed. In the bottom-level design problems, the system physics of failure (PoF) information is shared between system RBDO and system PHM design, which includes the failure modes considered in RBDO and the PHM design, the probability of

Fig. 3 A hierarchical resilience-driven system design framework

failure and the PHM efficiency for each failure mode. It is natural that with reliability and PHM efficiency being the focuses of the system RBDO and system PHM design, respectively, one should be able to predict the reliability and PHM efficiency levels for given components and PHM unit designs. This necessitates the developments of system reliability analysis and PHM analysis for these two bottom-level design problems which then complete the framework.

3.2 Resilience Allocation Problem (Top-Level). This section proposes the top-level design problem, referred to as the resilience allocation problem (RAP). Solving this design problem enables the optimal allocation of resilience levels—redundancy, reliability and PHM efficiency levels—to components.

3.2.1 Problem Formulation. The resilience of a system can be enhanced by increasing the degree of redundancy, reliability, and/or PHM efficiency at a component level. A rise in the resilience of a system, however, could lead to an increase in system LCC. Thus, based on the resilience definition above, a systematic trade-off can be formulated as an original RAP in this subtask. This original problem can be formulated as

$$\begin{aligned} \underset{\mathbf{r},\boldsymbol{\lambda},\mathbf{m}}{\text{minimize}} \quad & LCC(\mathbf{r}^t, \boldsymbol{\lambda}^t, \mathbf{m}) \\ \text{subject to} \quad & \Psi(\psi(\mathbf{r}^t, \boldsymbol{\lambda}^t, \mathbf{m})) \geq \Psi^t; \quad \mathbf{0} \leq \mathbf{r}^t, \boldsymbol{\lambda}^t \leq \mathbf{1} \\ & m_j^L \leq m_j \leq m_j^U, \quad j = 1, 2, \dots, N \end{aligned} \quad (3)$$

where LCC is the system life-cycle cost, Ψ and Ψ^t are system resilience and its target value, $\boldsymbol{\psi} = (\psi_1, \psi_2, \dots, \psi_N)^\mathrm{T}$ is an allocated resilience vector for all subsystems, N is the number of the subsystems, and the allocation decision variables include the target component-reliability vector $\mathbf{r}^t = (r_1^t, r_2^t, \dots, r_N^t)^\mathrm{T}$ with r_j^t being the target component-reliability of the jth subsystem, the target component-PHM efficiency vector $\boldsymbol{\lambda}^t = (\lambda_1^t, \lambda_2^t, \dots, \lambda_N^t)^\mathrm{T}$ with λ_j^t being the component-PHM efficiency of the jth subsystem, and the target component-redundancy vector $\mathbf{m} = (m_1, m_2, \dots, m_N)^\mathrm{T}$ with m_j being the target redundancy level of the jth subsystem. It is noted that, rather than considering PHM-relevant measures κ, Λ_P and Λ_D separately, we derive a combined measure, namely the component-PHM efficiency, defined as $\lambda \equiv \kappa \cdot \Lambda_P \cdot \Lambda_D$. Here λ is the measure of the capability of system restoration given a system failure event, which mathematically is the conditional probability of restoring the system through successful diagnosis, successful prognosis, and successful mitigation/recovery (M/R) action. For example, 0% λ represents one extreme case that the component does not have the restoration capability (no PHM unit is designed and integrated), whereas 75% λ means that, if there is a failure, the component will have 75% probability to restore its designed functionality through functioning of the PHM system. The proposed top-level RAP incorporates the PHM efficiency in design, where the reliability allocation can be considered as one special case in which PHM efficiencies for all components equal zero. Despite the loss of information to some extent, we argue that this manipulation greatly reduces the complexity of the problem as well as allows for an integrated treatment of a PHM unit in the subsequent system LCC analysis. This treatment is natural since, in the system level, we are interested in quantifying the counterpart of reliability in the resilience definition, i.e., the integrated capability (restoration) of a PHM unit to detect, predict and mitigate or recover from the system-wide effects of adverse events. We note that, in cases where we can build a detailed LCC model with the PHM-relevant measures (κ, Λ_P, and Λ_D) as model inputs, their separate consideration is quite possible but requires a greater amount of information regarding the LCC as well as leads to a higher complexity of the problem. The RAP in Eq. (3) makes it possible to optimally allocate target resilience levels—redundancy, reliability, and PHM efficiency levels—to components while meeting the target system resilience (Ψ^t). This problem is a mixed-integer nonlinear programming problem. It can be solved

using a genetic algorithm [48], ant colony optimization [49], particle swarm optimization [50], or other optimization techniques. Solving this problem will be computationally economic since the system resilience function Ψ can be analytically expressed in terms of the target component reliability vector $\mathbf{r}^t$, the component-PHM efficiency vector $\boldsymbol{\lambda}^t$ and the target component-redundancy vector $\mathbf{m}$. In what follows, the system resilience and LCC will be analyzed in details to evaluate the constraint and objective function in Eq. (3), respectively. For demonstration purposes, we intend to provide an example of a series-parallel system (see Fig. 4) which uses hypothetical data as its optimally allocated values for the target attributes (PHM efficiency and reliability levels) and the target structures (redundancy levels). As will be detailed in the subsequent section, these target attributes will be used later in the detailed design of components and PHM units.

3.2.2 Top-Level System Resilience Analysis. For different system configurations [51] (e.g., series-parallel, parallel-series, and general mixed system), the system resilience function can be built with the following two steps as:

Step 1: Derive the system resilience function in terms of subsystem resilience levels, i.e., $\Psi(\boldsymbol{\psi}) = \Psi(\psi_1, \dots, \psi_N)$. Since the system resilience is evolved from the system reliability, a reliability block diagram [52] and the analogy between the system reliability and resilience can be readily used to develop the analytic expression for the system resilience function.

Step 2: Build the subsystem resilience functions in terms of the target component-reliability, component-PHM efficiency and component-redundancy vectors, i.e., $\psi_j = \psi_j(r_j^t, \lambda_j^t, m_j)$ for $j = 1, 2, \dots, N$. Take a series-parallel system (see Fig. 4) as an example. Based on the generic resilience formula in Eq. (2), we can build the resilience function for the jth subsystem being a parallel system, expressed as

$$\psi_j \overset{\Delta}{=} R_j^t + \Lambda_j^t \cdot (1 - R_j^t) = 1 - (1 - r_j^t)^{m_j}(1 - \lambda_j^t)^{m_j} \quad (4)$$

where R_j^t and Λ_j^t are the jth subsystem reliability and PHM efficiency. In this series-parallel system, the components in the same subsystem possess the same reliability (r_j^t) because the components in parallel are identical and redundant, as are the PHM units.

3.2.3 Life-Cycle Cost (LCC) Analysis with PHM. In this study, we derive a LCC model by modifying and adding PHM relevant cost elements to an existing LCC model for deteriorating structural systems [53]. The LCC model consists of four cost elements: the expected initial development cost of components, the expected cost of preventive maintenance, the expected cost of corrective maintenance, and the expected development cost of PHM. Given the target component-reliability vector $\mathbf{r}^t$, the target component-PHM efficiency vector $\boldsymbol{\lambda}^t$, and the target component-redundancy vector $\mathbf{m}$, this LCC model can be expressed as

$$C(\mathbf{r}, \mathbf{m}, \boldsymbol{\lambda}) = C^I + C^{\mathrm{PM}} + C^{\mathrm{CM}} + C^{\mathrm{PHM}} \quad (5)$$
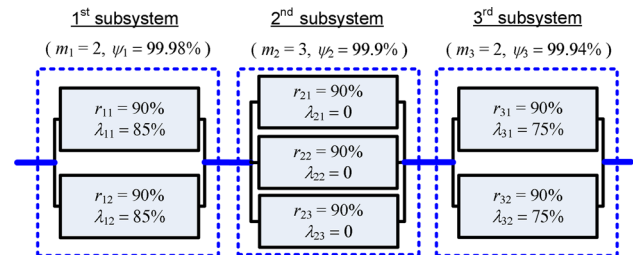

Fig. 4 Results of the resilience allocation problem for a series-parallel system

where C^I denotes the initial development cost of components, C^{PM} denotes the cost of preventive maintenance, C^{CC} denotes the cost of corrective maintenance, and C^{PHM} denotes the cost of PHM units. In what follows, the four cost elements will be discussed in details.

System development cost C^I. In the binary-state reliability-redundancy allocation problem, it is often assumed that there is an inverse power relationship between component cost and component failure rate [54,55]. Under the assumption of a constant failure rate, the initial development cost of the jth subsystem with m_j parallel components can be expressed as [54,55]

$$C_j^I = c_j^I\left(r_j^t\right) \cdot \left[m_j + \exp\left(\frac{m_j}{4}\right)\right], \text{ where } c_j^I(r_J^t) = \alpha_j^C\left(-\frac{T}{\ln\left(r_j^t\right)}\right)^{\beta_j^C} \tag{6}$$

where $c_j^I(r_j{}^t)$ is the cost function of a component in the jth subsystem, $c_j^I(r_j^t)\cdot m_j$ is the cost of components in the jth subsystem, an additional cost $c_j^I(r_j^t)\cdot\exp(m_j/4)$ accounts for the cost for interconnecting parallel components, T is the required system mission time, $\alpha_j{}^C$ and $\beta_j{}^C$ denote constants representing the physical characteristics of each component in the jth subsystem and can be determined based on the collected data of component cost and reliability. Therefore, the system initial development cost can computed as

$$C_j^I = \sum_{j=1}^{N} \alpha_j^C\left(-\frac{T}{\ln\left(r_j^t\right)}\right)^{\beta_j^C} \cdot \left[m_j + \exp\left(\frac{m_j}{4}\right)\right] \tag{7}$$

Preventive maintenance cost C^{PM}. That preventive maintenance occurs if PHM successfully detects critical system health states and accurately predicts the system RUL. As a function of the component reliability, subsystem redundancy and PHM efficiency, the preventive maintenance cost can be expressed as

$$C^{PM} = \sum_{j=1}^{N} m_j \lambda_j^t\left(1 - r_j^t\right)C_j^{PM} \tag{8}$$

where C_j^{PM} denotes the preventive maintenance cost of each component in the jth subsystem. The assumption here is that a preventive maintenance occurs when any component approaches its end of life predicted by the PHM and that all the components and PHM systems fail independently. We note that this cost element is associated with the primary benefit from the application of PHM to systems, i.e., failure avoidance [56]. System failures are very undesirable due to the extremely high failure costs, and the failure avoidance can be realized by capitalizing on PHM to provide an early anticipation and warning of future failure that allows preventative maintenance to be performed at a convenient place and time [56].

Corrective maintenance cost C^{CM}. The corrective maintenance occurs if PHM fails in detecting critical system health states and making an accurate prediction of the system RUL. As a function of the component reliability, subsystem redundancy and PHM efficiency, the corrective maintenance cost can be expressed as

$$C^{CM} = \sum_{j=1}^{N} m_j\left(1 - \lambda_j^t\right)\left(1 - r_j^t\right)C_j^{CM} \tag{9}$$

where C_j^{CM} denotes the corrective maintenance cost of each component in the jth subsystem and is far higher than the preventive maintenance cost C_j^{PM}. The assumption here is that a corrective maintenance occurs upon the failure of any component and that

all the components and PHM systems fail independently. In contrast to the preventive maintenance which always takes place before system failure, the corrective maintenance occurs after system failure and restores the system to a healthy state [57]. Since system failures incur very high costs, the corrective maintenance actions are rather undesirable, the minimization of which can be realized with PHM.

PHM unit cost C^{PHM}. The PHM unit cost is specifically the costs associated with developing PHM units to be integrated with components. In this study, the PHM unit cost will be formulated as a parametric model with the subsystem redundancy and component PHM efficiency as inputs. Inspired by the component cost function for reliability-redundancy allocation, shown in Eq. (3), we define the PHM unit cost as

$$C^{PHM} = \sum_{j=1}^{N} \alpha_j^{PHM}\left(-\frac{T}{\ln\left(r_j^t\right)}\right)^{\beta_j^{PHM}} \cdot m_j \tag{10}$$

where $\alpha_j{}^{PHM}$ and $\beta_j{}^{PHM}$ denotes constants representing the physical characteristics of each PHM unit in the jth subsystem. Prior to solving the optimization problem in Eq. (3), these constants can be determined based on the collected data of the PHM unit cost and efficiency. Since the PHM efficiency quantifies the probability of a PHM unit working properly and reliability quantifies the probability of a component functioning well, there is a similarity between these two probabilistic measures. Therefore, we derive the PHM unit cost model in Eq. (10) based on the component cost model [54,55] in Eq. (6) by replacing the target reliability r_j^t with the target PHM efficiency λ_j^t. It is noted that, in general, there is no interconnections between parallel PHM units. Therefore, unlike the component cost, the additional cost for interconnecting parallel elements is not considered in the PHM unit cost.

3.3 System RBDO (Bottom-Level). This section presents the bottom-level component design problem, referred to as the system reliability-based design optimization (RBDO). Solving this problem produces detailed designs of components in subsystems while ensuring the target reliability levels obtained in the top-level RAP.

3.3.1 System RBDO Formulation. To ensure the required system resilience Ψ, target component reliability levels optimally allocated in the top-level RAP will set the design constraints in this RBDO problem. This problem involves a vector $\mathbf{d}_j{}^C$ of detailed design variables for a component in the jth subsystem and can be formulated as

Minimize $C_j^I\left(\mathbf{d}_j^C\right)$

subject to $r_j^{\text{sys}} = \text{Pr}\left(E_j^{\text{sys}}\right) = \text{Pr}\left(\bigcup_{k=1}^{npj}\bigcap_{i \in P_k} G_j^i\left(\mathbf{x}_j^C;\mathbf{d}_j^C\right) \leq 0\right) \geq r_j^t$

$$\mathbf{d}_j^{C,L} \leq \mathbf{d}_j^C \leq \mathbf{d}_j^{C,U}$$

$$\tag{11}$$

where, the objective function $C_j{}^I$ is the refined model for the initial development cost of a component in the jth subsystem; $\mathbf{x}_j{}^C$ is the random vector; $\mathbf{d}_j{}^C = \boldsymbol{\mu}(\mathbf{x}_j{}^C)$ is the design vector; $G_j{}^i$ is the performance function of the ith constraint for $i = 1, \ldots, nc_j$, with nc_j being the number of constraints; r_j^{sys} is the system reliability level; E_j^{sys} is the system success event; P_k is the index set of constraints in the kth path set; np_j is the number of mutually exclusive path sets; r_j^t is the target system reliability level; $\mathbf{d}_j^{C,L}$ and $\mathbf{d}_j^{C,U}$ are the lower and upper bounds on $\mathbf{d}_j{}^C$, respectively. We note that a component in the jth subsystem possesses a "system" of multiple failure constraints. Thus, the "system" here should not be confused with the engineered system to which we apply the resilience-driven system design. It is also noted that the path set

formulation of the system reliability in Eq. (11) can represent any system structure (series, parallel, and mixed systems). In particular, the system success event E_j^{sys} of a series system contains only one path set in which the intersection operations are imposed over all constraints, expressed as

$$E_j^{\text{series}} = \bigcap_{i=1}^{nc_j} G_j^i\left(\mathbf{x}_j^C; \mathbf{d}_j^C\right) \leq 0 \qquad (12)$$

In this case, the component survives if and only if all of its constraints are satisfied. In contrast to a series system, a parallel system has multiple path sets with each being its component safety event, expressed as

$$E_j^{\text{parallel}} = \bigcup_{i=1}^{nc_j} G_j^i\left(\mathbf{x}_j^C; \mathbf{d}_j^C\right) \leq 0 \qquad (13)$$

In this case, the component survives if any of its constraints is satisfied.

In the past few decades, there has been a lot of serious research work in the component RBDO [1–6] with strong support from advanced numerical methods for component reliability analysis [7–10]. However, it is not until recently, to the best of our knowledge, that such research effort has been dedicated to the system RBDO, for which the system reliability analysis has been recognized as of great significance. The most recent works, we are aware of are [58] and [59] of which the former proposed a single-loop system RBDO formulation with the upper second-order bound to compute the probability of system failure and the latter used a matrix-based system reliability method to compute the system probability of failure in this system RBDO formulation. Through this literature survey, we intend to emphasize that any advanced system RBDO approach that will be newly developed can be readily incorporated into the proposed design framework. Despite a few technical advances in the system RBDO, the research in this field has been undergoing very slow progress mainly due to the stagnant status in the research of system reliability analysis. In the subsequent section, we will present the current research status on the system reliability analysis as well as introduce system reliability analysis for the bottom-level system RBDO.

3.3.2 System Reliability Analysis. Reliability analysis entails the computation of a multidimensional integration of a joint probability density function over a safety region

$$r = \int_{\Omega^s} f(\mathbf{x}) d\mathbf{x} \qquad (14)$$

where r denotes the structural reliability; $f(\mathbf{x})$ denotes the joint probability density function (PDF) of the vector of random variables; $\mathbf{x} = (x_1, x_2, \ldots, x_M)^{\text{T}}$ models uncertainty sources such as material properties, loads, and geometric tolerances; Ω^{S} denotes the safety domain. For component reliability analysis, the safety domain can be defined in terms of a limit-state function as $\Omega^{\text{S}} = \{\mathbf{x}: G(\mathbf{x}) < 0\}$, where $G(\mathbf{x})$ is a structural performance function. For system reliability analysis on a component in the jth subsystem involving nc_j performance functions, the safety domains can be expressed as

$$\Omega^s = \left\{\mathbf{x}_j^C : \bigcap_{i=1}^{nc_j} G_j^i\left(\mathbf{x}_j^C; \mathbf{d}_j^C\right) \leq 0\right\}, \qquad \text{series system}$$

$$\Omega^s = \left\{\mathbf{x}_j^C : \bigcup_{i=1}^{nc_j} G_j^i\left(\mathbf{x}_j^C; \mathbf{d}_j^C\right) \leq 0\right\}, \qquad \text{parallel system}$$

$$\Omega^s = \left\{\mathbf{x}_j^C : \bigcup_{k=1}^{np_j} \bigcap_{i \in P_k} G_j^i\left(\mathbf{x}_j^C; \mathbf{d}_j^C\right) \leq 0\right\}, \quad \text{mixed system}$$

$$(15)$$

In practice, however, it is extremely difficult to perform the multidimensional numerical integration even for component reliability

analysis when the number of random variables is relatively large. The search for efficient computational procedures to estimate the component reliability has resulted in a variety of numerical and simulation methods [7–10]. Compared with tremendous advances in component reliability analysis, the research in system reliability analysis has been stagnant, mainly due to two technical difficulties. First, it hard to derive an explicit formula for system reliability for given system redundancy. Second, even if system reliability is given explicitly, most numerical methods cannot effectively assess system reliability with high efficiency and accuracy.

3.4 System PHM Design (Bottom-Level). This section presents the bottom-level PHM unit design problem, referred to as the system PHM design. Solving this problem produces detailed designs of PHM units in subsystems while ensuring the target PHM efficiency levels obtained in the top-level RAP.

3.4.1 System PHM Design Formulation. To ensure the required system resilience (Ψ), we formulate a bottom-level system PHM design problem whose constraints are the target PHM efficiency levels optimally allocated in the top-level RAP. This problem involves a vector $\mathbf{d}_{pj}$ of detailed design variables for a PHM unit in the jth subsystem and can be formulated as

$$\begin{aligned}
\text{Minimize} \quad & C_j^{\text{PHM}}\left(\mathbf{d}_j^{\text{PHM}}\right) \\
\text{Subject to} \quad & \lambda_j\left(\mathbf{d}_j^{\text{PHM}}\right) \geq \lambda_j^t \\
& \mathbf{d}_j^{\text{PHM,L}} \leq \mathbf{d}_j^{\text{PHM}} \leq \mathbf{d}_j^{\text{PHM,U}}
\end{aligned} \qquad (16)$$

where the objective function C_j^{PHM} is the refined model for the development cost of a PHM unit in the jth subsystem; $\mathbf{d}_j^{\text{PHM}}$ is the design vector; λ_j is the PHM efficiency level; E_j^{sys}; r_j^t is the target system reliability level; $\mathbf{d}_j^{\text{PHM,L}}$ and $\mathbf{d}_j^{\text{PHM,L}}$ are the lower and upper bounds on $\mathbf{d}_j^{\text{PHM}}$, respectively. The development cost of a PHM unit mainly consists of two elements, that is, the sensing cost being proportioned to the number of sensors and the prognostic algorithm development cost. As mentioned in Sec. 3.2.1, the PHM efficiency can be further expressed as a multiplication $\lambda_j \equiv \kappa_j \cdot \Lambda_{Pj} \cdot \Lambda_{Dj}$, where the conditional probabilities Λ_{Pj} and Λ_{Dj} of correct prognosis and diagnosis vary with the design change and the conditional probability κ_j of correct maintenance remains fixed. Accordingly, the PHM design vector can be further decomposed into the diagnostics design vector $\mathbf{d}_j^D$ and prognostics design vector $\mathbf{d}_j^P$. In what follows, we intend to elaborate on these two categories of design variables.

Diagnostics design vector: The diagnostics design vector consists of design vectors for sensor network (SN) design to meet the required detectability level. Here, we use the term "detectability" to refer to the probability of correct diagnosis. In this work, $\mathbf{d}_j^D = (\mathbf{d}_j^{\text{TS}}, \mathbf{d}_j^{\text{LOC}})$ where $\mathbf{d}_j^{\text{TS}} = (d_{1j}^{\text{TS}}, d_{2j}^{\text{TS}}, \ldots, d_{Kj}^{\text{TS}})$ is a non-negative sensor type vector of which the kth element d_{kj}^{TS} represents the type (e.g., accelerometer, strain gauge, and acoustic sensor) of the kth sensor; and $\mathbf{d}_j^{\text{LOC}} = (d_{1j}^{\text{LOC}}, d_{2j}^{\text{LOC}}, \ldots, d_{Kj}^{\text{LOC}})$ is a real-valued sensor location vector of which the kth element d_{kj}^{LOC} is a three dimensional vector representing the sensor location of the kth sensor.

Prognostics design vector: The prognostics design vector consists of design vectors for prognostic algorithm design to meet the required prognostic accuracy level. Here, the term "prognostic accuracy" refers to the probability of correct prognostics. The design space for the prognostic algorithm design mainly consists of decision variables regarding the selection of algorithm types (e.g., the interpolation-based approaches [26,27], the extrapolation-based approach [60], and machine learning [61]) and control variables regarding the determination of algorithm parameters (e.g., numbers of training and testing units, and training termination criterion), i.e., $\mathbf{d}_j^P = (\mathbf{d}_j^{\text{TA}}, \mathbf{d}_j^{\text{PA}})$. Here, $\mathbf{d}_j^{\text{TA}} = (d_{1j}^{\text{TA}},$

$d_{2j}^{\text{TA}}, \ldots, d_{Qj}^{\text{TA}}$) is a vector of the binary decision variables regarding the selection of algorithm types: $d_{qj}^{\text{TA}} = 1$ if the prognostic algorithm of the qth type is applied to the jth subsystem, and $d_{qj}^{\text{TA}} = 1$ if this type of algorithm is not applied; and $\mathbf{d}_j^{\text{PA}} = (d_{1j}^{\text{PA}}, d_{2j}^{\text{PA}}, \ldots, d_{Zj}^{\text{PA}})$ is a real-valued vector of the parameter settings of selected algorithms.

As mentioned earlier, the PHM efficiency is mainly determined by the probabilities of correct diagnostics and prognostics, or the detectability and prognostic accuracy. In order to make the PHM design problem manageable, we intend to decouple the design problem associated with these two significant measures into two sub-problems, that is, a sensor network (SN) design problem to ensure a target probability of correct diagnostics or target detectability, and a prognostic algorithm design problem to achieve a target probability of correct prognostics or target prognostic accuracy. The SN design problem should be first solved to obtain an optimum SN satisfying the target detectability, followed by the prognostic algorithm design problem based on the sensory signals collected by the designed SN. In both sub-problems, the key PHM performance measures, detectability and prognostic accuracy, will be defined and measured in a nondeterministic manner. In what follows, the two design sub-problems will be elaborated with a focus on how to analyze the two PHM performance measures.

3.4.2 Sensor Network Design. This section presents the first PHM design sub-problem, detectability-based SN design, for health diagnostics of complex engineered systems. We first introduce the concept of detectability in a probabilistic manner that measures the diagnostic performance of a given SN. Subsequently, the detectability-based SN design framework is briefly discussed. In order to focus on the development of the RDSD framework, we intend not to delve deep into the SN design problem. Detailed information regarding this problem can be found in our complementary papers [62].

We propose the concept of detectability to quantify the capability of an SN to detect critical health states of complex engineered systems while accounting for multiple failure modes. With many failure modes obtained from the failure mode and effects analysis (FMEA) [63], the detectability can be expressed in a matrix form (see Fig. 5). The matrix is composed of true and detected failure modes on the vertical and horizontal axes, respectively, with the diagonal and off-diagonal elements being the probabilities of correct and incorrect detection, respectively. In what follows, we use D_i instead of D_{ii} to denote the ith diagonal element of the detectability matrix. The component detectability D_{i+1} (diagonal elements in Fig. 5) of the healthy condition HC ($i = 0$) or ith failure mode FM$_i$ ($i \geq 1$) can be defined as the probability of correct detection of the HC or FM$_i$ via an SN in the presence of the HC or FM$_i$. With the specified target detectability, these diagonal terms in the PoD matrix will then constitute $M + 1$ detectability con-

straints in the SN design process. Since theses detectability constraints involve the computation of multiple conditional probabilities, an efficient and accurate methodology for detectability analysis must be developed, which has been attempted with the support of computational models in our complementary papers [62].

In the SN design problem, the objective function is the sensing cost as a function of the sensor types and the number of sensors for each type. The design constraints are detectability requirements considering uncertainties presented in manufacturing and system operation processes. With all factors considered above, the SN design problem can be formulated as [62]

$$
\begin{aligned}
\text{Minimize} \quad & C_j^D \left(\mathbf{d}_j^D \right) \\
\text{subject to} \quad & D_{ij} \left(\mathbf{d}_j^D \right) \geq \Lambda_{Dj}^t, \ i = 1, 2, \ldots M + 1
\end{aligned}
\tag{17}
$$

where C_j^{PHM} is the sensing cost model for a PHM unit in the jth subsystem; $\mathbf{d}_j^D$ is the diagnostics design vector; D_{ij} is the detectability of the SN for the ith predefined health state, which is a function of the diagnostics design vector $\mathbf{d}_j^D$; Λ_{Dj}^t is the target detectability. The SN design optimization problem in Eq. (17) contains a discrete decision vector $\mathbf{d}_j^{\text{TS}}$ for the selection of sensor types, and continuous decision variables $\mathbf{d}_j^{\text{LOC}}$ for the sensor locations. Thus, it is formulated as a mixed-integer nonlinear programming (MINLP) problem [64], and heuristic algorithms such as genetic algorithms (GAs) can be employed to solve this optimization problem.

3.4.3 Prognostic Algorithm Design. This section introduces the second PHM design sub-problem, prognostic algorithm design, for health prognostics of complex engineered systems. In what follows, we will put the focus on the development of a systematic procedure to evaluate the prognostic accuracy of a given prognostic algorithm, while accounting for uncertainties presented in manufacturing and system operation processes. By evaluating the prognostic accuracy of candidate algorithms, we optimize the performance of these algorithms by adjusting their parameter settings. Upon the completion of performance optimization, we then select the one with the highest accuracy. We note that, since the development cost of a prognostic algorithm is dependent on the infrastructure and internal processes of the developer as well as on the implementation and testing of the algorithm, it is very difficult, if not possible, to trace back and identify all the cost elements incurred during the prognostic algorithm development. To simplify the problem in this study, we do not take into account any cost element in the prognostic algorithm design. The only objectives in the prognostic algorithm design are to optimize the algorithms and select the one with the highest prognostic accuracy.

Recently, many measures [61] have been developed for evaluating the performance of a prognostic algorithm; however, these measures do not take into account the unit-to-unit variation in a systematic manner. In this section, we attempt to derive an accuracy measure from the standpoint of probability. The measure can be evaluated based on the error data obtained over a population of prognostic components. The overall procedure to assess the prognostic accuracy Λ_{Pqj} of the algorithm of the qth type in the jth subsystem is detailed as follows:

Step 1: Apply the prognostic algorithm to a population of components in the jth subsystem and obtain the error vector consisting of errors in the RUL prediction of all components in the jth subsystem. The error in the RUL prediction is defined as the subtraction of the true RUL from the predicted RUL.

Step 2: Construct the error histogram based on the error vector and, if required for more convenient data representation, model the error histogram with an empirical PDF (error PDF in Fig. 6). An empirical PDF of the RUL prediction error e_{qj} can be constructed with the following three steps: (i) obtain optimum

Dij	HC	FM$_1$	FM$_2$	•••	FM$_M$
HC					
FM$_1$					
FM$_2$					
•••					
FM$_M$					

Fig. 5 Detectability matrix

distribution parameters for candidate distributions using the maximum likelihood method; (ii) perform quantitative hypothesis tests with the Chi-Square goodness-of-fit test for the candidate distribution types with the optimum distribution parameters obtained in the first step; and (iii) select the distribution type with the maximum p-value as the optimal distribution type for the RUL prediction error e_{qj}.

Step 3: The prognostic accuracy Λ_{Pqj} can be defined as the probability (shaded area in Fig. 6) that the prediction error lies within the error tolerance zone, expressed as

$$\Lambda_{Pqj} = \Pr\left(e_C \leq e_{qj} \leq 0\right) \approx \frac{1}{ns_j} \sum_{k=1}^{ns_j} I_{[e_C,0]}\left(e_{qj}^{(k)}\right) \qquad (18)$$

where e_C is the lower bound of the zone, ns_j is the number of prognostic components in the jth subsystem and $I[\cdot]$ is an indicator function of safe or fail state such that

$$I_{[e_C,0]}\left(e_{qj}^{(k)}\right) = \begin{cases} 1, & \text{if } e_{qj}^{(k)} \in [e_C, 0] \\ 0, & \text{otherwise} \end{cases} \qquad (19)$$

We note that, with a larger number of prognostic components, the resulting prognostic accuracy estimate better captures the uncertainties in manufacturing and system operation processes. However, in engineering practice, the number of prognostic components should be determined based on the amount of resources available. In the above equation, the upper bound of the zone is defined as the zero error, since a late prediction may cause a system failure. The lower bound must be carefully defined considering the cost of an M/R action, since an early prediction can lead to an unnecessary M/R action.

4 Aircraft Control Actuator Case Study

This section presents a case study for the design of a simplified aircraft control actuator. The aircraft control actuator considered is the electro-hydrostatic actuator (EHA) [66]. In this case study, we aim at demonstrating the RDSD framework by designing a highly resilient EHA with optimized reliability, PHM efficiency and redundancy. Hypothetical data will be used for demonstration purposes.

4.1 Problem Description.
The EHA (see Fig. 7), as a closed-loop, hydrostatic control system, mainly consists of an electronic control unit (ECU), a variable-speed electric motor (EM), a fixed-displacement hydraulic pump and a hydraulic piston actuator [67]. In the EHA, a variable-speed electric motor (typically DC) is used to drive a fixed-displacement hydraulic pump, which in turn, powers a hydraulic piston actuator. Compared to a conventional hydraulic actuator, the EHA can achieve higher energy efficiency (with on-demand usage) and positional accuracy with enhanced compactness. These advantages have led to the wide use of the EHA for flight surface actuation in today's commercial and military aircrafts. Failures of the EHAs in these safety
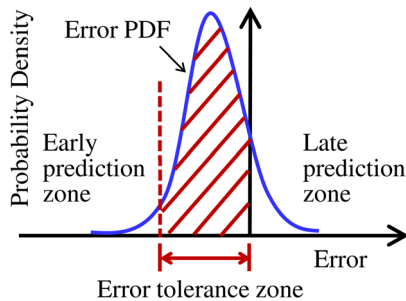
critical applications can be catastrophic, resulting in great loss of lives. Therefore, the EHA must be designed to achieve a sufficiently high reliability level. To this end, a common practice is to introduce a great deal of redundancy into the EHA (e.g., a triplex-redundant flight control system [68]). While a high redundancy level improves reliability, it results in a strikingly high life-cycle cost (LCC) to be incurred in development, operation, and maintenance processes. To reduce the LCC while still maintaining an equivalent reliability level, we apply the proposed RDSD framework to the EHA with an aim to compensate the redundancy reduction with the PHM technology. It is noteworthy that the RDSD framework leads to the possibility to implement this compensation in an optimum manner.

4.2 Top-Level RAP.
This subsection aims at demonstrating the top-level RAP in the RDSD framework by allocating a target system resilience into the target component-reliabilities, component-PHM efficiencies and component-redundancies of the four subsystems.

4.2.1 RAP Formulation.
Solving the top-level RAP will allocate a target system resilience level into the target resilience levels of the four subsystems. Assumptions under which this design problem is solved are listed as follows:

(1) The failure times all components considered in the example are exponentially distributed, leading to constant failure rates.
(2) PHM will detect critical system health states and predict system RUL through health diagnostics and prognostics
(3) The redundancy level of each subsystem should be no more than nine due to subsystem weight and volume constraints.
(4) All the components and PHM units fail independently. An observed failure is due to the loss of resilience, i.e., the failures of both a component and its associated PHM unit.

Based on the RAP formulation in Eq. (3), this problem is formulated as follows:

$$\text{find } \mathbf{r}^t = \left(r_1^t, r_2^t, r_3^t, r_4^t\right), \; \boldsymbol{\lambda}^t = \left(\lambda_1^t, \lambda_2^t, \lambda_3^t, \lambda_4^t\right),$$
$$\mathbf{m} = (m_1, m_2, m_3, m_4)$$

$$\text{to minimize } LCC = \sum_{j=1}^{4} \left(C_j^I + C_j^{\text{PM}} + C_j^{\text{CM}} + C_j^{\text{PHM}}\right) \qquad (20)$$

$$\text{subject to } \quad \Psi = \prod_{j=1}^{4}\left[1 - \left(1 - r_j^t\right)^{m_j}\left(1 - \lambda_j^t\right)^{m_j}\right] \geq \Psi^t$$

$$\mathbf{0} \leq \mathbf{r}^t, \boldsymbol{\lambda}^t \leq \mathbf{1}, \; \mathbf{1} \leq \mathbf{m} \leq \mathbf{9}$$

where LCC is the system life-cycle cost, Ψ and Ψ^t are system resilience and its target value, the lower and upper bounds for any target component-reliability or target component-PHM efficiency are 0 and 1, respectively, and the lower and upper bounds for any target component-redundancy are 1 and 9, respectively. The parameters for the cost models are listed in Table 1 and the system mission time $T = 1000$. The RAP problem is a mixed-integer
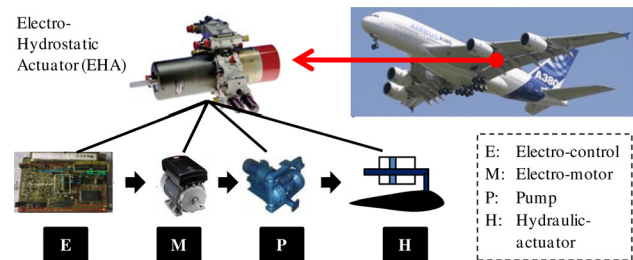

Fig. 6 Error PDF of RUL prediction

Fig. 7 An airplane control actuator with series-connected subsystems

Table 1 Model parameters for the EHA case study

Subsystem	$\alpha_j^C (\times 10^{-5})$	β_j^C	C_j^{PM}	C_j^{CM}	$\alpha_j^{PHM}(\times 10^{-6})$	β_j^{PHM}
1	0.5	1.5	2.5	7.5	3.3	1.5
1	0.8	1.5	5.0	15.0	5.3	1.5
2	1.0	1.5	6.5	19.5	6.7	1.5
3	0.7	1.5	12.5	37.5	4.7	1.5

nonlinear programming problem. To determine an optimum solution of the RAP problem, we employed a genetic algorithm of which the details will be presented in the Sec. 4.2.2.

4.2.2 Genetic Algorithm as the Optimization Solution Method. The top-level RAP in the RDSD framework is a mixed-integer nonlinear programming (MINLP) problem. To the best of the authors' knowledge, MINLP problems are generally solved by heuristic algorithms as an exhaustive search of the optimum solution is usually impractical. One of the most widely used algorithms is the so-called genetic algorithm (GA) [48] due to the following advantages: (i) the encoding scheme (binary or decimal encoding) in the GA leads to the flexibility to represent both continuous and discrete design variables and (ii) the search in the solution space for optimal solutions can be very efficient due to the use of fitness evaluation and genetic operator functions. Although the GA is employed to solve the top-level RAP, the computational cost for function evaluations can be negligible since the system LCC and resilience are computed through the evaluation of analytic models.

In the GA, each candidate solution is called a chromosome and a set of candidate solutions is called a population. The GA for solving the RAP in this case study employed the decimal encoding. The solution procedures are presented as follows [69]:

Step 1 (Initialization): Set the population size and maximum number of iterations as 500 and 100, respectively. Since one decimal digit represents one design variable in the RAP shown in Eq. (3), the length L of a chromosome reads: $L = 3N$. Set the upper and lower bounds for both component-reliability and component efficiency to 0 and 1, respectively. Set the upper and lower bounds for component-redundancy to 1 and 9, assuming the redundancy level should not be too high. Set the generation index $k_g = 1$ and randomly generate an initial population $\Gamma(1)$.

Step 2 (Evaluation): Evaluate the fitness function (ftn) for each chromosome in the current population $\Gamma(k_g)$. The fitness function used here is a composite of both the objective value (i.e., system LCC) and the penalty arising from the violation of the constraint (i.e., system resilience). Mathematically, the fitness function can be expressed as

$$\text{ftn} = \begin{cases} LCC(\mathbf{r}^t, \boldsymbol{\lambda}^t, \mathbf{m}), & \text{if } \Psi \geq \Psi^t \\ \inf, & \text{otherwise} \end{cases} \quad (21)$$

Step 3 (Parent selection): Select chromosomes from the current population based on their fitness values to form a new generation $\Gamma(k_g + 1)$. Here the roulette-wheel selection scheme is used. These chromosomes are called parent and will be used in the next step to generate new chromosomes in the new generation.

Step 4 (Crossover and mutation): Implement the two-point crossover operator with a crossover rate of 0.85 and the uniform mutation operator with a mutation rate of 0.10 to generate new chromosomes in the new population.

Step 5 (Termination check): If the generation index k_g exceeds the maximal number of iterations, terminate the iteration and report the solution. Otherwise, increase the generation index: $k_g = k_g + 1$, and go back to Step 2.

4.2.3 Results and Discussion. We would like to investigate scenarios with different target system resilience levels. First let us look at the scenario in which the target system resilience Ψ^t is set as 0.90. The optimum solution is shown in Table 2. It can be seen that the incorporation of PHM by the proposed RDSD reduces the system redundancy from $\mathbf{m} = (3, 2, 3, 2)$ to $\mathbf{m} = (2, 2, 2, 1)$. As a consequence, the system LCC decreases from 73.6301 under the traditional design (without PHM) to 38.3416 under the RDSD (with PHM). It is noted that, even though the target component-reliabilities are relatively low for both traditional design (below 0.8500) and RDSD (below 0.7500), the incorporation of redundant components (traditional design and RDSD) and PHM (RDSD) still leads to high subsystem reliabilities (above 0.90). Finally, the system resilience levels under both optimum designs read 0.9000, which just satisfies the system resilience requirement.

Raising the target system resilience to 0.95 and 0.99, respectively, we then obtained two sets of optimal designs, which are listed in Table 3 and Table 4, respectively. We observe that, in order to meet higher target system resilience level, more components are used with higher component-reliabilities and PHM efficiencies. Compared with the traditional design, the RDSD still yields optimum designs with much lower LCCs by considering PHM in the early design stage. The target component-reliabilities and component-PHM efficiencies allocated in this RAP can serve as design specifications for bottom-level system RBDO and PHM design that will be detailed in the Secs. 4.3 and 4.4.

4.3 Bottom-Level System RBDO. This subsection aims at demonstrating the bottom-level system RBDO in the RDSD framework. We intend to determine the optimal design of the hydraulic actuator satisfying the target reliability obtained from the RAP with the target system resilience Ψ^t being 0.99. The success event of the actuator is considered as a series system success event consisting of four component success events.

4.3.1 Description of EHA Model. In order to investigate the performance of different actuator designs, we employed an EHA model built in a 1D multidomain simulation platform LMS Imagine.Lab AMESim [70]. A simplified schematic of the EHA model is shown in Fig. 8, where each submodel (e.g., motor, pump and actuator) is composed of a set of algebraic and differential equations accounting for linear and nonlinear effects such as friction and leakage. Here, a variable-speed DC motor drives a fixed-displacement hydraulic pump, which supplies oil to the actuator. A proportional controller controls the flow rate by varying the speed of the electric motor. An accumulator is used to prevent cavitation and compensate leakage loss with refeeding valves.

Table 2 Optimum results of traditional design and RDSD with $\Psi^t = 0.90$

Subsystem	Traditional design (without PHM)					RDSD (with PHM)				
	r_j^t	m_j	λ_j^t	LCC	Ψ	r_j^t	m_j	λ_j^t	LCC	Ψ
1	0.7371	3	0	73.6301	0.9000	0.6291	2	0.6721	38.3416	0.9000
2	0.8088	2	0	—	—	0.6412	2	0.6682	—	—
3	0.7287	3	0	—	—	0.6519	2	0.6732	—	—
4	0.8292	2	0	—	—	0.7363	1	0.7679	—	—

Table 3 Optimum results of traditional design and RDSD with $\Psi^t = 0.95$

	Traditional design (without PHM)					RDSD (with PHM)				
Subsystem	r_j^t	m_j	λ_j^t	LCC	Ψ	r_j^t	m_j	λ_j^t	LCC	Ψ
1	0.7901	3	0	82.2774	0.9500	0.6152	2	0.6448	45.9357	0.9500
2	0.7731	3	0	—	—	0.6437	2	0.6644	—	—
3	0.7872	3	0	—	—	0.6486	2	0.6677	—	—
4	0.8574	2	0	—	—	0.7539	2	0.7423	—	—

The pressure relief valves aim at preventing excessive pressure build-up in the hydraulic lines. As the flow encounters the actuator, the fluid pressure increases. The pressure difference between the two actuator chambers results in an actuation force, and thus a linear piston motion. A mechanical arm (not shown in Fig. 8) then transforms the piston motion to an equivalent aileron angle while taking into account the aileron inertia.

4.3.2 System RBDO Formulation. For the system RBDO, we used the weight of the actuator to build the objective function and

the control performance to formulate the reliability constraints. Regarding the control performance, we intended to take into account two aspects: timeliness and robustness. We applied a step request (1 cm) on the piston position at the time $t = 0.5$ s and a resistive torque (2000 N·m) at the time $t = 1.0$ s to test the control timeliness and robustness, respectively. The piston position response is shown in Fig. 9, where the reliability constraints G_1 and G_2 are treated as timeliness-relevant constraints and G_3 and G_4 robustness-relevant. Specifically, this system RBDO problem can be formulated as follows:

$$
\begin{aligned}
&\underset{x}{\text{Minimize}} \quad C(\mathbf{x}) = \omega \cdot V_s(d_p, l_s) + (1-\omega) \cdot V_r(d_r, l_s) \\
&\text{where} \quad \omega = 0.098, \; V_s = l_s \cdot \pi(d_p/2)^2, \; V_r = l_s \cdot \pi(d_r/2)^2 \\
&\text{Subject to} \quad r^{\text{sys}} = \Pr(E^{\text{sys}}) = \Pr\left(\bigcap_{i=1}^4 G_i(\mathbf{x}) \leq 0\right) \geq r^t \\
&\qquad G_1 = \int_0^2 |Y(t) - Y_{ref}(t)| dt - e_{nc} \qquad \text{(normal control error)} \\
&\qquad G_2 = \underset{0.5 \leq t \leq 2}{\arg \min}\{|Y(t) - Y_{ref}(t)| \leq \varepsilon_{tol,s}\} - t_{c,s} \quad \text{(stabilization time)} \\
&\qquad G_3 = \int_2^4 |Y(t) - Y_{ref}(t)| dt - e_{pc} \qquad \text{(disturbed control error)} \\
&\qquad G_4 = \underset{2 \leq t \leq 4}{\min}\{|Y(t) - Y_{ref}(t)|\} - \varepsilon_{tol,d} \qquad \text{(disturbed steady-state error)} \\
&\qquad G_5 = \eta - d_r/d_p \qquad \text{(rod-to-piston diameter ratio)}
\end{aligned}
\tag{22}
$$

where the critical normal control error $e_{nc} = 0.20$ cm·s, the stabilization error tolerance $\varepsilon_{tol,s} = 0.03$ cm and is used to determine whether a stable state is achieved, the critical stabilization time $t_{c,s} = 0.90$ s, the critical perturbed control error $e_{np} = 0.05$ cm·s, the steady-state error tolerance under a disturbance $\varepsilon_{tol,d} = 0.04$ cm and the rod-to-piston diameter ratio $\eta = 1/3$. To avoid having a weak rod relative to a piston, we also add the fifth constraint G_5 in Eq. (22) which ensures that the rod-to-piston ratio exceed a certain level. The following two design variables are considered: the piston diameter d_p and the rod diameter d_r. These design variables

are assumed to follow normal distributions with their standard deviations, initial values and lower and upper bounds detailed in Table 5. Three model parameters (i.e., the leakage coefficient β, viscous friction coefficient v, and the stroke length l_s) are considered as random noise variables with their statistical information summarized in Table 6. In summary, five random design and noise variables are considered in this study.

4.3.3 Results. The adaptive-sparse polynomial chaos expansion (PCE) method with $4nv + 1$ (= 21) univariate samples was

Table 4 Optimum results of traditional design and RDSD with $\Psi^t = 0.99$

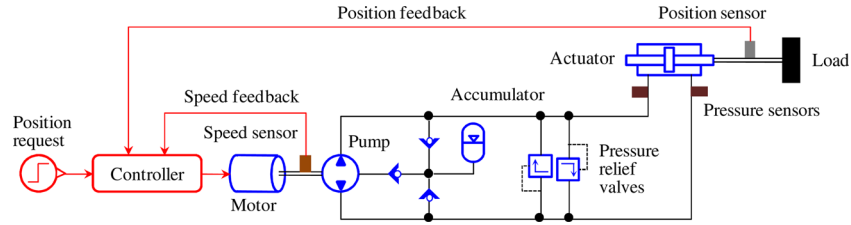|	Traditional design (without PHM)					RDSD (with PHM)				
Subsystem	r_j^t	m_j	λ_j^t	LCC	Ψ	r_j^t	m_j	λ_j^t	LCC	Ψ
1	0.8102	4	0	111.6017	0.9900	0.6488	3	0.6772	55.0199	0.9900
2	0.7745	4	0	—	—	0.6483	3	0.7049	—	—
3	0.7850	4	0	—	—	0.6567	2	0.8014	—	—
4	0.8411	3	0	—	—	0.7720	2	0.7678	—	—

Fig. 8   Schematic of an (EHA) model

carried out to evaluate the objective function, system reliability and their sensitivities at any design iteration, without considering the bivariate polynomial basis functions [71]. The sensitivities of the objective function and system reliability with respect to the two design variable were computed using a finite difference method (FDM). The perturbed values of the objective function and system reliability were estimated based on approximate stochastic response surfaces (PCE) with perturbed design variables, without requiring gradients of the original weight or displacement functions. A perturbation size of 0.1% is employed in this study.

The design optimization problem was solved using a gradient-based optimization technique (e.g., sequential quadratic optimization). The histories of the design parameters, objective function, component reliabilities and system reliability are shown in Table 7. At the initial design, the system reliability r^{sys} severely violated the reliability requirement due to the relatively low component reliabilities r_3 and r_4. After six design iterations, the optimum design was found where the system reliability requirement was satisfied. Overall, the adaptive-sparse PCE method required 126 simulations for system RBDO. After the optimization, the direct Monte Carlo simulation (MCS) with 10,000 random samples was employed to verify the reliability results at the optimum design. The component reliabilities r_1, r_2, r_3, r_4, and r_5 and system reliability r^{sys} were estimated by the MCS as 95.36%, 94.40%, 85.99%, 89.74%, 93.65%, and 77.24%, respectively.

4.4 Bottom-Level System PHM Design. This subsection is dedicated to demonstrating the bottom-level system PHM design in the RDSD framework. We intend to design a data-driven prognostic algorithm for the actuator leakage prognostics by identifying the most appropriate algorithm from an algorithm pool. We assume that the PHM unit can successfully identify the incipient leakage degradation of the actuator among various possible failure modes ($\Lambda_D = 1$) and that, upon a correct prognosis event, the M/R maintenance actions can fully restore the reliability of the actuator ($\kappa = 1$).

4.4.1 Prognostic Data Generation. The failure mode considered in this study is the actuator cross-line leakage which is relatively common in practice [72,74]. The wear of the piston seal causes an increase of internal cross-port leakage and thus an increase in the leakage coefficient of the actuator. Thus, the cross line leakage was realized by increasing the leakage coefficient of the actuator. The end of life is defined as the time when the actuator leakage reaches ten times its initial value. We note that, for demonstration purposes, this study only considers a single failure mode, but the same idea can be readily extended to cases with multiple failure modes.

Since it is very difficult, if not impossible, to obtain direct measurements of the leakage coefficients of actuators, indirect measurements are most often used to diagnose the health condition and predict the RULs of actuators [72,74]. In particular, the stabilized piston displacement after disturbance (measured by a position sensor) and the stabilized rotary speed of the motor shaft after disturbance (measured by a rotary speed sensor) could characterize the actuator leakage degradation before any irreparable damage occurs [72]. Thus, this case study employs these two sensory signals of an EHA to predict the RULs of actuators. To model the trajectory of increase in leakage over time, this study uses a damage propagation model with an exponential form as Ref. [74]

$$\beta(t) = \beta_0 + b_E(\exp(a_E t) - 1) \qquad (23)$$

where β_0 is the initial leakage coefficient; a_E and b_E are the model parameters; t is the cycle time. The initial Young's modulus E_0 follows the same normal distribution with β (see Table 6). The model parameters a_E and b_E are independent and normally distributed with means 0.01 and 1.2×10^{-3}, each of which has a 10% coefficient of variation. The random parameters considered in this study are listed in Table 5 and Table 6, which include the material properties as well the geometries of the actuator. The uncertainties in the two sensory signals propagated from these uncertain parameters will be accounted for when generating prognostic data. The prognostic data generation were conducted under the optimal actuator design obtained in the bottom-level system design (see Sec. 4.3).

Since data-driven prognostic approaches require a large amount of prognostic data, it is computationally expensive, if not impossible, to simply run the simulation to generate every data point. To overcome this difficulty, this study employed the univariate decomposition method that only uses a certain number of univariate sample points to construct the response surface for a general multivariate response function while achieving good accuracy [75]. Since this study employed two sensory signals, namely the stabilized piston displacement after disturbance and the stabilized rotary speed of the motor shaft after disturbance, the data generation requires the construction of two responses surfaces. Specifically, the data generation process involves four sequentially executed procedures:

Step 1: Obtain univariate sample points from the dynamic simulation in LMS Imagine.Lab AMESim to construct response surfaces, along the damage propagation path, that approximate the two sensory measurements as functions of random variables detailed in Table 5 and Table 6. We used four univariate sample points for each random variable. The piecewise linear spline was used as the numerical scheme for the response surface construction.

Table 5   Random design variables for the hydraulic actuator model

Design variable	Distri. type	Lower bound	Initial des.	Upper bound	Std. dev.
d_p (mm)	Normal	55.0	62.0	75.0	3.5
d_r (mm)	Normal	10.0	22.0	30.0	1.0

Table 6   Random noise variables for the hydraulic actuator model

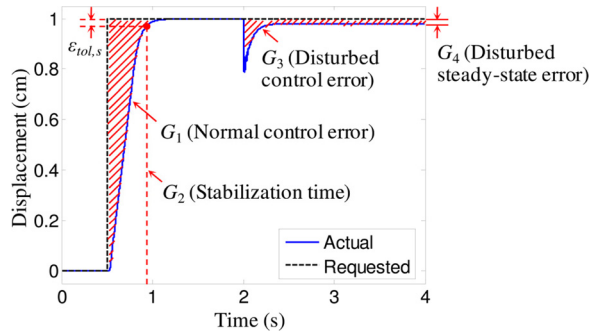| Random variable	Distri. type	Mean	Std. dev.
B (L/min/Bar)	Normal	1.2×10^{-3}	6.0×10^{-5}
υ (N·s/m)	Normal	5.0×10^{3}	2.5×10^{-2}
l_s (mm)	Normal	50.0	2.5

Fig. 9 Piston position response under a step request and resistive torque

Step 2: Generate 400 random samples of β_0, a_E, and b_E and use these samples in conjunction with Eq. (23) to produce 400 damage propagation paths, of which 200 paths were assigned to the training units and the rest to the testing units.

Step 3: Interpolate, based on the constructed response surfaces, the two sensory measurements for a given set of randomly generated geometries and material properties and damage propagation paths and repeatedly execute this process for 400 times to obtain the training data set with 200 training units and the testing data set with 200 testing units.

Step 4: Add measurement noise following a zero mean normal distribution to both the training and testing data sets to finalize the data generation.

The two simulated measurements are plotted against the adjusted cycle index, defined as the subtraction of the cycle-to-failure from the actual operational cycle, for all 200 training units in Fig. 10, where we can clearly observe monotonic lifetime trends for both measurements.

4.4.2 Description of Prognostic Algorithms. This section provides a brief overview of the five selected data-driven prognostic algorithms: Method 1—a similarity-based interpolation (SBI) approach with the relevance vector machine (RVM) as the regression technique (RVM-SBI) [26,76,77], Method 2—SBI with the relevance vector machine (SVM) as the regression technique (SVM-SBI) [26,78], Method 3—SBI with the least-square exponential fitting (Exp-SBI) [26], Method 4—a Bayesian linear regression (BLR) with the least-square quadratic fitting (Quad-BLR) [60], and Method 5—a recurrent neural network (RNN) approach (RNN) [61,79]. A data processing scheme with a generic health index system is used for the first four algorithms while a data processing scheme with a simple normalization scheme for the last algorithm. These five algorithms represent the current state-of-art in data-driven prognostics and cover a wide range of

techniques that include the interpolation (Methods 1–3), extrapolation (Method 4) and machine learning (Method 5).

For the construction of the virtual health index in Methods 1–3, the system failure matrix $\mathbf{Q}_0$ was created with the sensory data in a system failure condition, $0 \leq L \leq 4$, while the system healthy matrix $\mathbf{Q}_1$ with those in a system healthy condition, $L > 250$. The RVM employed a linear spline kernel function with the initial most probable hyper-parameter vector for kernel weights $\mathbf{\alpha}_m = [1 \times 10^4, \dots, 1 \times 10^4]$ and the initial most probable noise variance $\sigma_m^2 = 1 \times 10^{-4}$. In the SVM, a Gaussian kernel function is used with the parameter settings as: the regularization parameter $C = 10$ and the parameter of the ε-insensitive loss function $\varepsilon = 0.10$. In the RNN training, the two normalized sensory signals were used as the multidimensional inputs of the RNN and the RUL at the corresponding cycle was used as the output. The implementation details can be found in Ref. [61]. In the RNN architecture, the numbers of the input, recurrent and output units are $|I| = 2$, $|R| = 4$, and $|O| = 1$.

4.4.3 Results. Table 8 summarizes the prognostic accuracy of the five candidate algorithms as well as the detailed information regarding the empirical error PDFs. The lower bound e_C of the error tolerance zone was set as -35 cycles. Among the five candidate algorithms, RNN yields the highest prognostic accuracy of 0.790 on the testing data set, a 43.6% improvement over the second best algorithm, Exp-SBI, whose prognostic accuracy reads 0.550. To further investigate this accuracy gap, we plotted the RUL predictions by the two algorithms for 200 testing units in Fig. 11(a) and their error PDFs in Fig. 11(b). It can be observed from both plots that RNN consistently gives early RUL predictions while Exp-SBI is prone to produce RUL predictions being randomly distributed around zero. Therefore, RNN provides higher accuracy in spite of a larger variance and, with failure prevention being the main goal of PHM, one would select RNN among the candidate algorithms to have moderately early RUL predictions. Indeed, it is noted that only RNN satisfies the target component-PHM efficiency 0.7678 obtained in Sec. 4.2 with the assumption of perfect diagnostics and M/R actions. Finally, we note that, by capitalizing on PHM, the EHA is capable of detecting, predicting and mitigating or recovering from the actuator leakage, and thus achieves the resilience characteristics intended by the underlying idea of RDSD, namely the optimal restoration of system capacity and performance.

5 Conclusion

This paper presents a novel design framework, namely resilience-driven system design (RDSD), to incorporate resilience characteristics into complex engineered systems. This new design framework consists of three hierarchical tasks, namely the top-level RAP, the bottom-level system RBDO and the bottom-level
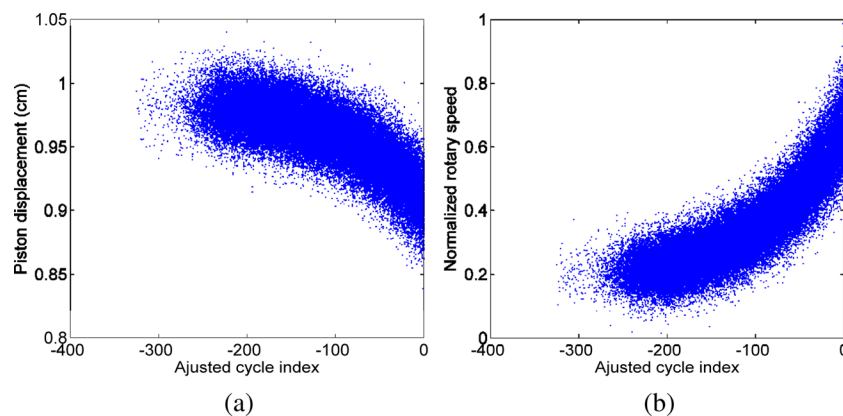

Fig. 10 Simulated measurements by piston displacement sensor (*a*) and rotary speed sensor (*b*) for the hydraulic actuator model
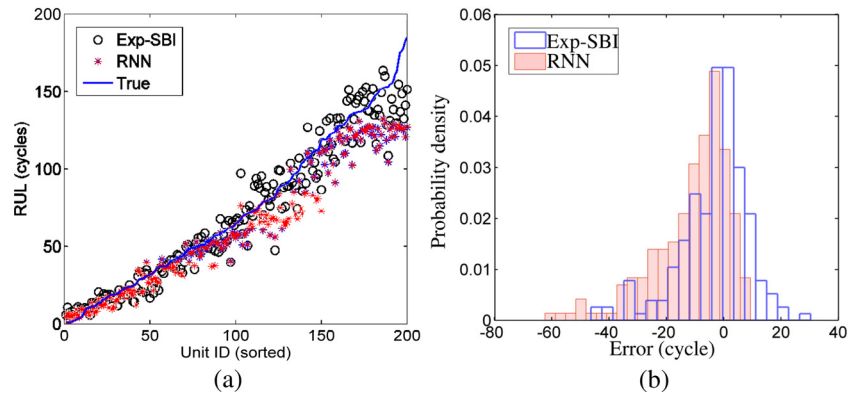
Fig. 11 RUL prediction results (*a*) and error PDFs (*b*) for the hydraulic actuator model

Table 7 Design history of the hydraulic actuator model

| Iter. | Design variables | | r_1 | r_2 | r_3 | r_4 | r_5 | r^{sys} | Obj. |
	d_p	d_r							
0	62.0000	22.0000	0.9985	0.9978	0.4955	0.5350	0.8053	0.3093	3.2015×10^4
1	65.8472	24.5219	0.9819	0.9767	0.7695	0.8162	0.9522	0.7136	3.8062×10^4
2	66.7479	24.7483	0.9694	0.9617	0.8309	0.8699	0.9471	0.7620	3.8916×10^4
3	66.9844	24.7694	0.9640	0.9551	0.8459	0.8826	0.9429	0.7698	3.9075×10^4
4	67.1807	24.6941	0.9586	0.9479	0.8607	0.8947	0.9314	0.7707	3.9044×10^4
5	67.1847	24.7177	0.9587	0.9479	0.8604	0.8944	0.9331	0.7717	3.9088×10^4
6	67.1617	24.7268	0.9594	0.9488	0.8587	0.8929	0.9346	0.7720	3.9092×10^4
Opt	67.1617	24.7268	0.9594	0.9488	0.8587	0.8929	0.9346	0.7720	3.9092×10^4

Table 8 Prognostic accuracy and empirical error PDF results for the hydraulic actuator model

Algorithm	Prognostic accuracy	Distri. Type	Mean (cycle)	Std. dev. (cycle)	Parameters for nonnormal distributions
RVM-SBI	0.480	Weibull	− 2.66	12.14	$\alpha_1 = 49.22, \beta_1 = 4.15$[a]
SVM-SBI	0.430	Weibull	− 3.40	14.91	$\alpha_2 = 60.10, \beta_2 = 4.12$[b]
Exp-SBI	0.550	Normal	− 3.17	12.03	—
Quad-BLR	0.125	Weibull	10.62	12.76	$\alpha_4 = 63.82, \beta_4 = 5.31$[c]
RNN	0.790	Weibull	− 12.10	13.07	$\alpha_5 = 55.17, \beta_5 = 4.35$[d]

[a]$(e_1 \geq − 47.36)$.
[b]$(e_2 \geq − 57.96)$.
[c]$(e_4 \geq − 48.17)$.
[d]$(e_5 \geq − 62.35)$.

system PHM design. The top-level RAP incorporates the trade-off decisions regarding the component-reliability, component-PHM efficiency, and component-redundancy into the system-level design for an optimum integration of PHM with minimum LCC. The bottom-level system RBDO determines an optimal component design while ensuring the optimally allocated target component-reliability from the top-level RAP. Following the system RBDO, the bottom-level system PHM design derives an optimal PHM unit design for the optimal component design while meeting the optimally allocated PHM efficiency from the top-level RAP. The proposed RDSD framework, featured with a rigorous theoretical basis and analysis and design strategy of engineering resilience, is expected to ensure highly resilient system designs under various loading/environmental conditions and system-wide effects of adverse events while considerably reducing systems' LCC. The proposed RDSD framework is demonstrated with a simplified aircraft control actuator design problem, in which the incorporation of PHM significantly reduces the system LCC and the detailed component and PHM unit designs respectively satisfy the target component-reliability and

component-PHM efficiency. Future works under contemplation include the verification of the proposed framework using testing data from a real complex engineered system, the consideration of multiple failure modes for the system PHM design and the integration of diagnostics design (SN design) with prognostics design (prognostic algorithm design).

Nomenclature

r_j^t = target component-reliability of the *j*th subsystem
m_j = component redundancy level of the *j*th subsystem

E_{sf} = system failure event
E_{cd} = correct diagnosis event
E_{cp} = correct prognosis event
E_{mr} = M/R action success event
R_j^t = target system reliability of the jth subsystem
Λ_D = conditional probabilities of the correct diagnosis
Λ_j^t = target PHM efficiency of the jth subsystem
Λ_P = conditional probabilities of the correct prognosis
κ = conditional probabilities of the M/R action success
λ_j^t = target component-PHM efficiency of the jth subsystem
ψ_j = resilience of the jth subsystem
Ψ = system resilience
Ψ^t = target system resilience
ρ = system capacity restoration
BLR = Bayesian linear regression
CAS = complex adaptive systems
CBM = condition-based maintenance
CM = condition monitoring
ECU = electronic control unit
EHA = electro-hydrostatic actuator
EM = electric motor
FMEA = failure mode and effects analysis
GA = genetic algorithm
LCC = life-cycle cost
MCS = Monte Carlo simulation
M/R = mitigation/recovery
PCE = polynomial chaos expansion
PDF = probability density function
PHM = prognostics and health management
RAP = resilience allocation problem
RBDO = reliability-based design optimization
RDSD = resilience-driven system design
RNN = recurrent neural network
RUL = remaining useful life
RVM = relevance vector machine
SBI = similarity based interpolation
SN = sensor network
SVM = support vector machine

References

[1] Du, X., and Chen, W., 2004, "Sequential Optimization and Reliability Assessment Method for Efficient Probabilistic Design," ASME J. Mech. Des., **126**(2), pp. 225–233.
[2] Youn, B. D., Choi, K. K., and Du, L., 2005, "Enriched Performance Measure Approach (PMA+) for Reliability-Based Design Optimization," AIAA J., **43**(4), pp. 874–884.
[3] McDonald, M., and Mahadevan, S., 2008, "Reliability-Based Optimization with Discrete and Continuous Decision and Random Variables," ASME J. Mech. Des., **130**(6), 061401.
[4] Kim, C., and Choi, K. K., 2008, "Reliability-Based Design Optimization Using Response Surface Method with Prediction Interval Estimation," ASME J. Mech. Des., **130**(12), 121401.
[5] Youn, B. D., and Wang, P., 2008, "Bayesian Reliability-Based Design Optimization Using Eigenvector Dimension Reduction (EDR) Method," Struct. Multidiscipl. Optim., **36**(2), pp.107–123.
[6] Wang, P., Youn, B. D., Xi, Z., and Artemis, K., 2009, "Bayesian Reliability Analysis with Evolving, Insufficient and Subjective Data Sets," ASME J. Mech. Des., **131**(11), 111008.
[7] Rahman, S, and Xu, H., 2004, "A Univariate Dimension-Reduction Method for Multi-Dimensional Integration in Stochastic Mechanics," Probab. Eng. Mech., **19**(4), pp. 393–408.
[8] Youn, B. D., Choi, K. K., and Yi, K., 2005, "Performance Moment Integration (PMI) Method for Quality Assessment in Reliability-based Robust Design Optimization," Mech. Based Des. Struct. Mach., **33**(2), pp.185–213.
[9] Youn, B. D., Xi, Z., and Wang, P., 2008, "Eigenvector Dimension Reduction (EDR) Method for Sensitivity-Free Uncertainty Quantification," Struct. Multidiscip. Optim., **37**(1), pp. 13–28.
[10] Xiong, F., Greene, S., Chen, W., Xiong, Y., and Yang, S., 2010, "A New Sparse Grid Based Method for Uncertainty Propagation," Struct. Multidiscip. Optim., **41**(3), pp. 335–349.
[11] Christer, A. H., and Waller, W. M., 1984, "Delay Time Models of Industrial Inspection Maintenance Problems," J. Oper. Res. Soc., **35**(5), pp. 401–406.
[12] Makis, V., Yimin, Z., and Jardine, A. K. S., 2006, "Adaptive State Detection of Gearboxes under Varying Load Conditions Based on Parametric Modeling," Mech. Syst. Signal Process., **20**(1), pp. 188–221.
[13] Chinnam, R. B., and Baruah, P., 2003, "A Neuro-Fuzzy Approach for Estimating Mean Residual Life in Condition-Based Maintenance Systems," Int. J. Mater. Prod. Technol., **20**(1–3), pp. 166–179.
[14] Lin, C. C., and Tseng, H. Y., 2005, "A Neural Network Application for Reliability Modeling and Condition-Based Predictive Maintenance," Int. J. Mater. Prod. Technol., **25**(1–2), pp. 174–179.
[15] Alguindigue, I. E., Loskiewicz-Buczak, A., and Uhrig, R. E., 1993, "Monitoring and Diagnosis of Rolling Element Bearings Using Artificial Neural Networks," IEEE Trans. Ind. Electron. Control Instrum., **40**(2), pp. 209–217.
[16] Ebersbach, S., Peng, Z., and Kessissoglou, N. J., 2006, "The Investigation of The Condition and Faults of a Spur Gearbox Using Vibration and Wear Debris Analysis Techniques," Wear, **260**(1–2), pp. 16–24.
[17] Dimla, D. E., 2000, "Sensor Signals for Tool-Wear Monitoring in Metal Cutting Operations - a Review of Methods," Int. J. Mach. Tools Manuf., **40**(8), pp. 1073–1098.
[18] Martin, K. F., 1994, "Review by Discussion of Condition Monitoring and Fault Diagnosis in Machine Tools," Int. J. Mach. Tools Manuf., **34**(4), pp. 527–551.
[19] Bartoletti, C., Desiderio, M., Di Carlo, D., Fazio, G., Muzi, F., Sacerdoti, G., and Salvatori, F., 2004, "Vibroacoustic Techniques to Diagnose Power Transformers," IEEE Trans. Power Delivery, **19**(1), pp. 221–229.
[20] Bengtsson, C., 1996, "Status and Trends in Transformer Monitoring," IEEE Trans. Power Delivery, **11**, pp. 1379–1384.
[21] Booth, C., and McDonald, J. R., 1998, "The Use of Artificial Neural Networks for Condition Monitoring of Electrical Power Transformers," Neurocomputing, **23**, pp. 97–109.
[22] Luo, J., Pattipati, K. R., Qiao, L., and Chigusa, S., 2008, "Model-Based Prognostic Techniques Applied to a Suspension System," IEEE Trans. Syst. Man Cybern., Part A. Syst. Humans, **38**(5), pp. 1156–1168.
[23] Gebraeel, N., and Pan, J., 2008, "Prognostic Degradation Models for Computing and Updating Residual Life Distributions in a Time-Varying Environment," IEEE Trans. Device Mater. Reliab., **57**(4), pp. 539–550.
[24] Gebraeel, N., Elwany, A., and Pan, J., 2009, "Residual Life Predictions in the Absence of Prior Degradation Knowledge," IEEE Trans. Device Mater. Reliab., **58**(1), pp. 106–117.
[25] Schwabacher, M., 2005, "A Survey of Data-Driven Prognostics", Proceedings of AIAA Infotech at Aerospace Conference, Arlington, VA.
[26] Wang, T., Yu, J., Siegel, D., and Lee, J., 2008, "A Similarity-Based Prognostics Approach for Remaining Useful Life Estimation of Engineered Systems," International Conference on Prognostics and Health Management, Oct. 6–9, Denver, CO.
[27] Zio, E., and Di Maio, F., 2010, "A Data-Driven Fuzzy Approach for Predicting the Remaining Useful Life in Dynamic Failure Scenarios of a Nuclear Power Plant," Reliab. Eng. Syst. Saf., **95**(1), pp. 49–57.
[28] Goebel, K., Eklund, N., and Bonanni, P., 2006, "Fusing Competing Prediction Algorithms for Prognostics," Proceedings of IEEE Aerospace Conference, New York.
[29] Saha, B., Goebel, K., Poll, S., and Christophersen, J., 2009, "Prognostics Methods for Battery Health Monitoring Using a Bayesian Framework," IEEE Trans. Instrum. Meas., **58**(2), pp. 291–296.
[30] Yanagisawa, A., and Kojima, T., 2006, "Degradation of InGaN Blue Light-Emitting Diodes under Continuous and Low-Speed Pulse Operations," Microelectron. Reliab., **43**(6), pp. 977–980.
[31] Hausler, K., Zeimer, U., Sumpf, B., Erbert, G., and Trankle, G., 2008, "Degradation Model Analysis of Laser Diodes," J. Mater. Sci.: Mater. Electron., **9**, pp. 160–164.
[32] Klasson, T. K., and Just, E. M., 1999, "Computer Model for Prediction of PCB Dechlorination and Biodegradation Endpoints," Proceedings the 5th International Symposium on In Situ and On-Site Bioremediation, San Diego, CA, April 19–22.
[33] Shrive, N. G., 2005, "Intelligent Structural Health Monitoring: a Civil Engineering Perspective," IEEE Trans. Syst. Man Cybern., **2**(10–12), pp. 1973–1977.
[34] Aven, T., 1996, "Condition-based Replacement Policies—A Counting Process Approach," Reliab. Eng. Syst. Saf., **51**(3), pp. 275–281.
[35] Grall, A., Bérenguer, C., and Dieulle, L., 2002, "A Condition-Based Maintenance Policy for Stochastically Deteriorating Systems," Reliab. Eng. Syst. Saf., **76**(2), pp. 167–180.
[36] Deloux, E., Castanier, B., and Berenguer, C., 2009, "Predictive Maintenance Policy for a Gradually Deteriorating System Subject to Stress," Reliab. Eng. Syst. Saf., **94**(2), pp. 418–431.
[37] Bodden, D. S., Hadden, W., Grube, B. E., and Clements, N. S., 2005, "PHM as a Design Variable in Air Vehicle Conceptual Design," Proceedings of 2005 IEEE Aerospace Conference, Mar. 5–12, Big Sky, MT, pp. 1–11.
[38] Webb, C. T., 2007, "What Is The Role Of Ecology in Understanding Ecosystem Resilience?," BioScience, **57**(6), pp. 470–471.
[39] Hartvigsen, G., Kinzig, A., and Peterson, G., 1998, "Complex Adaptive Systems: Use and Analysis of Complex Adaptive Systems in Ecosystem Science: Overview of Special Section," Ecosystems, **1**(5), pp. 427–430.
[40] Kerkhoff, A. J., and Enquist, B. J., 2007, "The Implications of Scaling Approaches for Understanding Resilience and Reorganization in Ecosystems," BioScience, **57**(6), pp. 489–499.
[41] Luthar, S. S., Cicchetti, D., and Becker, B., 2000, "The Construct of Resilience: a Critical Evaluation and Guidelines for Future Work," Child Dev., **71**(3), pp. 543–562.
[42] Bonanno, G. A., Moskowitz, J. T., Papa, A., and Folkman, S., 2005, "Resilience to Loss in Bereaved Spouses, Bereaved Parents, and Bereaved Gay Men," J. Pers. Soc. Psychol., **88**(5), pp. 827–843.

[43] Bonanno, G. A., and Galea, S., 2007, "What Predicts Psychological Resilience After Disaster?" The Role of Demographics, Resources, and Life Stress," J. Consult Clin. Psychol., **75**(5), pp. 671–682.

[44] Luthar, S. S., *Poverty and Children's Adjustment* (Sage, Newbury Park, CA, 1999).

[45] Sheffi, Y., *The Resilient Enterprise: Overcoming Vulnerability for Competitive Enterprise* (MIT Press, Cambridge, MA, 2005).

[46] Hollnagel, E., Woods, D. D., and Leveson, N. (eds.), 2006, *Resilience Engineering: Concepts and Precepts*, Ashgate, Aldershot, UK.

[47] Hollnagel, E., 2006, "Achieving System Safety by Resilience Engineering," *The 1*st *IET International Conference on System Safety*, June 6–8, London, United Kingdom, pp. 184–195.

[48] Hsieh, Y., Chen, T., and Bricker, D., 1998, "Genetic Algorithms for Reliability Design Problems," Microelectron. Reliab., **38**(10), pp. 1599–1605.

[49] Liang, Y.-C., and Smith, A. E., 2004, "An Ant Colony Optimization Algorithm for the Redundancy Allocation Problem (RAP)," IEEE Trans. Device Mater. Reliab. **53**(3), pp. 417–423.

[50] Coelho, L. S., 2009, "An Efficient Particle Swarm Approach for Mixed-Integer Programming in Reliability-Redundancy Optimization Applications," Reliab. Eng. Syst. Saf., **94**(4), pp. 830–837.

[51] Kuo, W., and Zuo, M. J., *Optimal Reliability Modeling: Principles and Applications* (John Wiley, Hoboken, NJ, 2002).

[52] Rausand, M., and Høyland, A., 2003, *System Reliability Theory: Models, Statistical Methods, and Applications*, 2nd ed., Wiley-Interscience, Hoboken, NJ.

[53] Frangopol, D. M., Lin, K.-Y., Estes, A., 1997, "Life-Cycle Cost Design of Deteriorating Structures," J. Struct. Eng., **123**(10), pp. 1390–1401.

[54] Tillman, F. A., Hwang, C. L., and Kuo, W., 1977, "Determining Component Reliability and Redundancy for Optimum System Reliability," IEEE Trans. Device Mater. Reliab., **26**(3), pp. 162–165.

[55] Dhingra, A. K., 1992, "Optimal Apportionment of Reliability and Redundancy in Series Systems under Multiple Objectives," IEEE Trans. Device Mater. Reliab., **41**(4), pp. 576–582.

[56] Feldman, K., Jazouli, T., and Sandborn, P., 2009, "A Methodology for Determining the Return on Investment Associated with Prognostics and Health Management," IEEE Trans. Device Mater. Reliab., **58**(2), pp. 305–316.

[57] Nilsson, J., and Bertling, L., 2007, "Maintenance Management of Wind Power Systems Using Condition Monitoring Systems—Life Cycle Cost Analysis for Two Case Studies," IEEE Trans. Energy Convers., **22**(1), pp. 223–229.

[58] Liang, J., Mourelatos, Z., and Nikolaidis, E., 2007, "A Single-Loop Approach for System Reliability-Based Design Optimization," ASME J. Mech. Des., **129**(12), pp. 1215–1224.

[59] Nguyen, T. H., Song, J., and Paulino, G. H., 2010, "Single-Loop System Reliability-Based Design Optimization Using Matrix-Based System Reliability Method: Theory and Applications," ASME J. Mech. Des., **132**, 011005.

[60] Coble, J. B., and Hines, J. W., 2008, "Prognostic Algorithm Categorization with PHM Challenge Application," IEEE, International Conference on Prognostics and Health Management, Oct. 6–9, Denver, CO.

[61] Saxena, A., Celaya, J., Balaban, E., Goebel, K., Saha, B., Saha, S., and Schwabacher, M., 2008, "Metrics for Evaluating Performance of Prognostic Techniques," International Conference on Prognostics and Health Management, June 20–23, Denver, CO.

[62] Heimes, F. O., 2008, "Recurrent Neural Networks for Remaining Useful Life Estimation," IEEE, International Conference on Prognostics and Health Management, Oct. 6-9, Denver, CO.

[63] Wang, P., Youn, B. D., and Hu, C., 2010, "A Generic Sensor Network Design Framework Based on A Detectability Measure," *ASME International Design Engineering Technical Conferences and Computers and Information in Engineering Conference (IDETC/CIE)*, Aug. 15–18, Montreal, Quebec, Canada.

[64] Kmenta, K., and Ishii, K., 2005, "Scenario-Based Failure Modes and Effects Analysis Using Expected Cost," ASME J. Mech. Des., **126**(6), pp. 1027–1035.

[65] Adjiman, C. S., Androulakis, I. P., and Floudas, C. A., 2000, "Global Optimization of Mixed-Integer Nonlinear Problems," Trans. Am. Inst. Chem. Eng., **46**(9), pp. 1769–1797.

[66] Frischermeier, S., 1997, "Electrohydrostatic Actuators for Aircraft Primary Flight Control - Types, Modelling and Evaluation," Proceedings of the Fifth Scandinavian International Conference on Fluid Power, May 28–30, Linköping, Sweden.

[67] Botten, S., Whitley, C., and King, A., 2000, "Flight Control Actuation Technology for Next-Generation All-Electric Aircraft," *Technology Review Journal—Millenium Issue*, Fall/Winter.

[68] Osder, S., 1999, "Practical View of Redundancy Management Application and Theory," J. Guid. Control Dyn., **22**(1), pp. 12–21.

[69] Gen, M., and Cheng, R., *Genetic Algorithms and Engineering Optimization* (John Wiley & Sons, New York, 2000).

[70] The LMS Imagine.Lab AMESim Suite, 2010. http://www.lmsintl.com/imagine-amesim-1-d-multi-domain-system-simulation.

[71] Hu, C., and Youn, B. D., 2011, "Adaptive-Sparse Polynomial Chaos Expansion for Reliability Analysis and Design of Complex Engineering Systems," Struct. Multidiscip. Optim., **43**(3), pp. 419–442.

[72] Crowther, W. J., Edge, K. A., Burrows, C. R., Atkinson, R. M., and Wollons, D. J., 1998, "Fault Diagnosis of a Hydraulic Actuator Circuit using Neural Networks an Output Vector Space Classification Approach," Proc. Inst. Mech. Eng.—Part I: J. Syst. Control Eng., **212**(11), pp. 57–68.

[73] An, L., and Sepehri, N., 2006, "Hydraulic Actuator Leakage Quantification Scheme Using Extended Kalman Filter and Sequential Test Method," *Proceedings of American Control Conference*, June 14–16, p. 6.

[74] Saxena, A., and Goebel, K., 2008, "Damage Propagation Modeling for Aircraft Engine Run-To-Failure Simulation," *IEEE, International Conference on Prognostics and Health Management*, Oct. 6–9, Denver, CO.

[75] Xu, H., and Rahman, S., 2005, "Decomposition Methods for Structural Reliability Analysis," Probab. Eng. Mech., **20**(3), pp. 239–250.

[76] Tipping, M. E., 2001, "Sparse Bayesian Learning and the Relevance Vector Machine," J. Mach. Learn. Res., **1**, pp. 211–244.

[77] Wang, P., and Youn, B. D., 2009, "A Generic Bayesian Framework for Real-Time Prognostics and Health Management (PHM)," AIAA 2009-2109, 50th AIAA/ASME/ASCE/AHS/ASC Structures, Structural Dynamics, and Materials Conference, May 4–7, Palm Springs, CA.

[78] Smola, A. J., and Schölkopf, B., 2004, "A Tutorial on Support Vector Regression," Stat. Comput., **14**(3), pp. 199–222.

[79] Cernansky, M., Makula, M., and Cernansky, L., 2007, "Organization of the State Space of a Simple Recurrent Network before and after Training on Recursive Linguistic Structures," Neural Networks, **20**(2), pp. 236–244.